
Devonshire, Ian M. and Burston, James and Xu, Luting and Lillywhite, A. and Prior, M.J. and Watson, David J.G. and Greenspon, C.M. and Iwabuchi, Sarina J. and Auer, Dorothee P. and Chapman, Victoria (2017) Manganese-enhanced magnetic resonance imaging depicts brain activity in models of acute and chronic pain: a new window to study experimental spontaneous pain? NeuroImage, 157 . pp. 500-510. ISSN 1095-9572

NeuroImage 157 (2017) 500–510

Contents lists available at ScienceDirect

NeuroImage

journal homepage: www.elsevier.com/locate/neuroimage

# Manganese-enhanced magnetic resonance imaging depicts brain activity in models of acute and chronic pain: A new window to study experimental spontaneous pain?

I.M. Devonshire[a,b,1], J.J. Burston[a,b,1], L. Xu[a,b], A. Lillywhite[a,b], M.J. Prior[c], D.J.G. Watson[b], C.M. Greenspon[b], S.J. Iwabuchi[c,d], D.P. Auer[a,c,d], V. Chapman[a,b,*]

[a] Arthritis Research UK Pain Centre, University of Nottingham, UK
[b] School of Life Sciences, University of Nottingham, UK
[c] Medical Imaging Unit, School of Medicine, University of Nottingham, UK
[d] Neuroradiology, Nottingham University Hospitals Trust, Nottingham NG7 2UH, UK

ARTICLE INFO

*Keywords:*
Nociception
fMRI
Manganese
On-going pain
Osteoarthritis

ABSTRACT

Application of functional imaging techniques to animal models is vital to understand pain mechanisms, but is often confounded by the need to limit movement artefacts with anaesthesia, and a focus on evoked responses rather than clinically relevant spontaneous pain and related hyperalgesia. The aim of the present study was to investigate the potential of manganese-enhanced magnetic resonance imaging (MEMRI) to measure neural responses during on-going pain that underpins hyperalgesia in pre-clinical models of nociception. As a proof of concept that MEMRI is sensitive to the neural activity of spontaneous, intermittent behaviour, we studied a separate positive control group undergoing a voluntary running wheel experiment.

In the pain models, pain behaviour (weight bearing asymmetry and hindpaw withdrawal thresholds (PWTs)) was measured at baseline and following either intra-articular injection of nerve growth factor (NGF, 10 μg/50 μl; acute pain model, n=4 rats per group), or the chondrocyte toxin monosodium iodoacetate (MIA, 1 mg/50 μl; chronic model, n=8 rats per group), or control injection. Separate groups of rats underwent a voluntary wheel running protocol (n=8 rats per group). Rats were administered with paramagnetic ion $Mn^{2+}$ as soluble $MnCl_2$ over seven days (subcutaneous osmotic pump) to allow cumulative activity-dependent neural accumulation in the models of pain, or over a period of running. T1-weighted MR imaging at 7 T was performed under isoflurane anaesthesia using a receive-only rat head coil in combination with a 72 mm volume coil for excitation.

The pain models resulted in weight bearing asymmetry (NGF: 20.0 ± 5.2%, MIA: 15 ± 3%), and a reduction in PWT in the MIA model (8.3 ± 1.5 g) on the final day of assessment before undergoing MR imaging. Voxel-wise and region-based analysis of MEMRI data did not identify group differences in T1 signal. However, $MnCl_2$ accumulation in the VTA, right Ce amygdala, and left cingulate was negatively correlated with pain responses (greater differences in weight bearing), similarly $MnCl_2$ accumulation was reduced in the VTA in line with hyperalgesia (lower PWTs), which suggests reduced regional activation as a result of the intensity and duration of pain experienced during the 7 days of $MnCl_2$ exposure. Motor cortex T1-weighted signal increase was associated with the distance ran in the wheel running study, while no between group difference was seen. Our data suggest that on-going pain related signal changes identified using MEMRI offers a new window to study the neural underpinnings of spontaneous pain in rats.

## Introduction

Chronic pain disorders are debilitating, costly to society and have a complex pathophysiology (Tracey and Bushnell, 2009). Imaging techniques are important tools in the study of chronic pain (Lee and Tracey, 2013) but the vast majority of imaging studies of pain focus on evoked responses rather than spontaneous pain, but the brain regions activated by painful stimuli only partially overlap with those attributed to

* Corresponding author at: Arthritis Research UK Pain Centre, University of Nottingham, UK.
*E-mail address:* victoria.chapman@nottingham.ac.uk (V. Chapman).
[1] These authors contributed equally to the work undertaken.

http://dx.doi.org/10.1016/j.neuroimage.2017.06.034
Received 13 March 2017; Accepted 16 June 2017
Available online 17 June 2017

spontaneous pain (Parks et al., 2011), with a shift to emotional brain regions such as the amygdala and putamen (Kulkarni et al., 2007; Howard et al., 2011; Cottam et al., 2016). Conversely experimental hyperalgesia induces upregulation of brain responses within known pain processing areas with significantly higher BOLD responses to cutaneous noxious stimuli in the dorsal anterior cingulate, bilateral anterior, left posterior insula, right inferior parietal lobule, right middle frontal gyrus and left striatum, based on a recent meta-analysis of 11 studies (Tanasescu et al., 2016).

Animal models offer a number of benefits to the study of chronic pain, including the evaluation of novel treatments and differentiation of underlying mechanisms across different types of pain (Borsook and Becerra, 2011). The clinical relevance of the models of pain employed, type of assessments of pain response (evoked versus on-going responses) and longitudinal testing of the models are fundamental to optimise translational validity of the findings (Tappe-Theodor and Kuner, 2014). Greater emphasis of pre-clinical studies on the neural mechanisms underlying spontaneous pain may provide targets for more effective treatment options in chronic pain disorders. Functional magnetic resonance imaging (fMRI) provides an important snap-shot of brain regional activity, however commonly images are acquired from anaesthetised animals which, whilst acceptable for the acquisition of structural data, can limit the information obtained from functional scans (Borsook and Becerra, 2011; Martin et al., 2006; Martin, 2014; Abaei et al., 2016) if not entirely obscure activity (Thompson et al., 2014). Although imaging in awake animals is feasible, it may introduce other confounds such as stress (Thompson and Bushnell, 2012). An alternative fMRI-based approach is to administer an activity-dependent magnetic resonance (MR) contrast agent with a long half-life whilst the animals are awake to capture waking-state activity when the animal is anaesthetised during read out. $Mn^{2+}$ is a paramagnetic ion usually delivered as $MnCl_2$, which acts as a $Ca^{2+}$ analog and has a half-life of approximately 12 days in cortex (Chuang et al., 2009). $MnCl_2$ enters excitable cells via voltage-, receptor- or non-specific calcium channels and can be used for functional contrast related to neural activity (Silva et al., 2004; Boretius and Frahm, 2011) that is not dependent on a haemodynamic response. Although early studies using acute $MnCl_2$ administration had issues with toxicity (Olanow, 2004; Wolf and Baum, 1983; Silva et al., 2004; Jackson et al., 2011), slower longer-term administration has overcome this problem (Eschenko et al., 2010; Hoch et al., 2013; Mok et al., 2012).

Here we have sought to address both the over-reliance on evoked data in pain studies and the limitations of acquiring imaging data from anaesthetised animals. We hypothesized that manganese-enhanced magnetic resonance imaging (MEMRI) could identify regional brain activity related to ongoing pain behaviour in the rat. To address this question a short-lasting, versus longer-lasting, model of pain behaviour was employed. Nerve growth factor (NGF) is a pro-inflammatory molecule that produces a relatively short lasting sensitization and activation of sensory nerves following subcutaneous or intra-articular injection into the knee joint (Lewin et al., 2014). The second model employed is associated with a longer-lasting period of nociceptive behaviour following the intra-articular injection of the chondrocyte toxin monosodium iodoacetate (MIA), which replicates aspects of the joint pathology and pain exhibited by human OA (Guingamp et al., 1997; Combe et al., 2004). Herein we report the first use of MEMRI to examine regional uptake of $MnCl_2$, and, by inference, activity, in the brain following a period of short term nociceptive behaviour or versus sustained nociceptive pain behaviour in separate groups of rats. As a control, the effects of running on regional uptake of $MnCl_2$ were also quantified in a separate group of rats.

## Methods

The experiments described were approved by the local University ethical committee and all procedures were performed and specifically licensed following approval by the UK Home Office and in accordance with the Animals (Scientific Procedures) Act 1986 which incorporates Council Directive 2010/63EU of the European Parliament. Adult male Sprague Dawley rats (n=32) were used (Charles River, Margate, UK) and were housed on a reversed 12-h dark/artificial-light cycle in conventional cages at a temperature of 21 ± 2 °C and 55% humidity; food and water were available ad libitum.

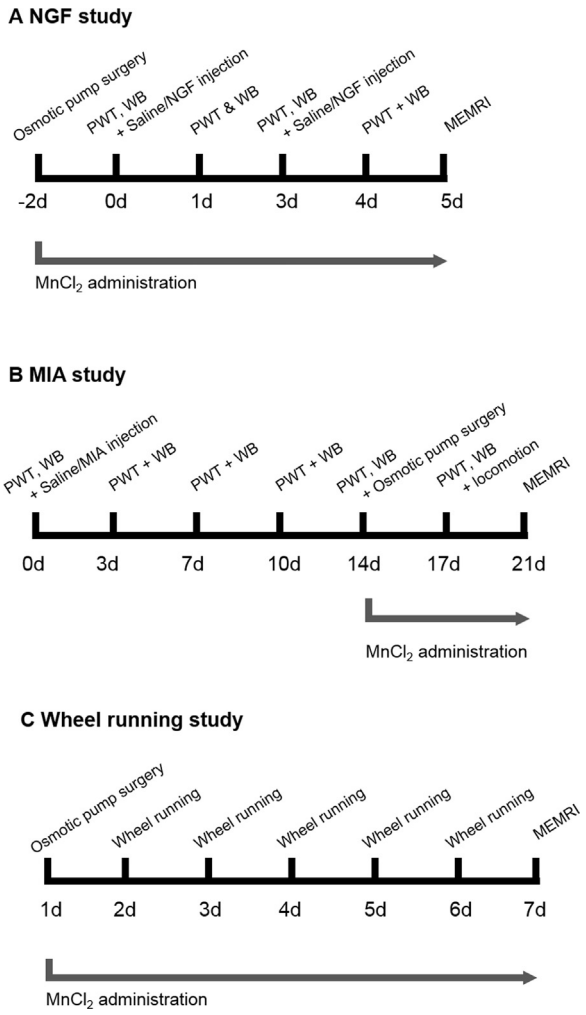


**Fig. 1.** Timelines of the acute intra-articular nerve growth factor (A) and chronic intra-articular monosodium iodoacetate (B) pain models and also the running wheel study (C). In the NGF model, two intra-articular injections of either saline or NGF were given on days (d) 0 and 3. In the MIA model, a single intra-articular injection of saline or MIA was given on d0. Behavioural pain assessments were performed as indicated and comprised of hindpaw withdrawal thresholds (PWT), weight bearing difference (WB) and locomotion. In the running wheel study rats had access to a running wheel for 3 h per day for 5 days before imaging. In all three studies the period of $MnCl_2$ (80 mg/kg) administration by implanted osmotic pump is indicated by gray arrows.

### *Intra-articular injections*

Rats were randomly assigned to a treatment group briefly anesthetised with isoflurane (2.5–3% in $O_2$) and received either intra-articular injection through the infra-patellar ligament of the left knee of nerve growth factor (NGF 10 μg/50 μl in saline; Sigma, Gillingham, UK; dose based on (Ashraf et al., 2014), n=4), monosodium iodoacetate (MIA; 1 mg /50 μl in saline; Sigma; dose based on (Sagar et al., 2010), n=8), or saline (50 μl; n=12) using a 30 gauge hypodermic needle. For the NGF group, a second identical injection of NGF was given three days after the first injection (Fig. 1). Accuracy of injection was confirmed at the end of the study by the un-blinding of pain behaviour data. All

surgical procedures were performed in a blinded fashion, under sterile conditions in an animal procedure room away from animal holding areas. The experimental unit was a single animal.

*Behavioural testing*

After intra-articular injection, rats were maintained under the same conditions as during the pre-operative period. The posture and behaviour of rats was carefully monitored following recovery from the anaesthesia and throughout the study. Weight gain, changes in hindlimb weight distribution and mechanical paw withdrawal thresholds (PWTs) were measured by an experimenter blinded to treatment immediately prior to intra-articular injection (day 0, baseline) and at regular intervals (days 1, 3 and 4 in the NGF short-lasting pain study in which a second intra-articular injection of NGF was given on day 3, and on days 3–17 in the MIA longer-lasting pain study; Fig. 1) until the day of imaging. Spontaneous locomotion and rearing activity was measured in the MIA-treated rats on day 17. The tester was blind to the treatment at the time of testing. Behavioural tests were always performed between 8 a.m. and noon.

Healthy rats distribute their weight evenly between both paws, and changes in weight distribution are used as an indicator of discomfort and associated pain. Weight-distribution through the left (ipsilateral) and right (contralateral) hindpaw were assessed using an incapacitance tester (Linton Instrumentation, Diss, UK), as previously described (Sagar et al., 2014). Three weight bearing measures were taken at each time point, measures from the left hindpaw were subtracted from right hindpaw and converted to a percentage change (0% signifies equal weight distribution while > 0% represents a shift of weight distribution to the uninjured limb). Mechanical PWTs were assessed using calibrated von Frey monofilaments (Semmes-Weinstein monofilaments of bending forces 1, 1.4, 2, 4, 6, 8, 10, 15 and 26 g; Linton Instrumentation) applied to the plantar surface of the hind paw in ascending order of bending force. Each hair was applied three times for approximately 2–3 s periods or until a withdrawal response was evoked using established criteria (Chaplan et al., 1994). After a response, the paw was retested with the monofilaments in descending order until no response occurred, at which point the monofilaments were again applied in ascending order until the response could once again be evoked. The monofilament that evoked this final reflex was noted as the PWT.

Spontaneous locomotor and rearing activity was recorded during a 1 h period in an unfamiliar Perspex arena (39 cm × 23.5 cm × 24.5 cm) using a computerised infra-red activity system (Photobeam Activity System, San Diego Instruments, San Diego, USA) under dimmed lighting. Horizontal ambulatory activity was measured as the consecutive interruption of two adjacent lower beams, while the number of rears was measured by interruption of a separate layer of upper beams. Cumulative beam-breaks were automatically recorded in 5 min time bins for the test duration (Watson et al., 2012).

*Voluntary wheel running in rats*

In an additional group of adult male Sprague Dawley rats wheel running was used as a positive control based on a similar published MEMRI study (Eschenko et al., 2010). Following one week of acclimatisation rats were provided with a running wheel for 3 h duration for 5 nights. A wheel running system with a diameter of 27 cm with a magnetic detector and a wireless bicycle computer with anti-interference wireless recorder were synchronised and calibrated such that one full rotation was set to a distance of 84.7 cm (wheel circumference = π * diameter).

Following training and habituation of rats to the running wheel system, rats were assigned to either a running group or non-running group (n= 8 rats per group). One rat was placed into a cage with a single running wheel for three hours on five consecutive nights (20:00 to 23:00) before being returned to home cage. Distance ran was recorded and rats that showed consistent running ( > 200 m per session) for four or more sessions were selected for the running group. The non-running group of rats (n=8) were not given access to a functional running wheel system (apparatus was present but could not rotate) and therefore the distance these rats ran on the wheel was zero meters.

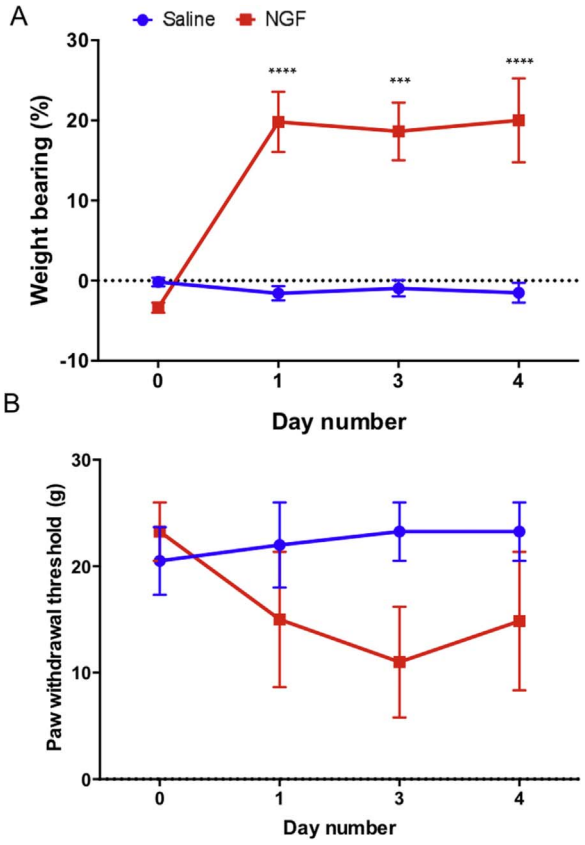


**Fig. 2.** Pain behaviour was assessed immediately before and 24 h after each intra-articular injection of NGF (10 μg/50 μl, n=4, red line) or saline (50 μl, n=4, blue line). (A) There was significant weight bearing asymmetry at all time points after the first NGF injection on day 0, compared to injection of saline. Weight bearing asymmetry was sustained but not further increased following the second injection of NGF on day 3. (B) There was no change in hindpaw withdrawal thresholds following intra-articular injection of NGF or saline at either day 0 or 3. Data were analysed using a two-way ANOVAs (drug × time) and Sidak's multiple comparison post-hoc test; error bars represent standard error of the mean; *** $p < 0.001$, **** $p < 0.0001$.

*Osmotic pump implantation for $MnCl_2$ administration*

$MnCl_2 \cdot (H_2O)2$ (VWR, Lutterworth, UK) was administered chronically via an osmotic pump (model 2001, 200 μl volume; Alzet, Cupertino, USA). Implantation of osmotic pumps was performed seven days before imaging (day −2 in the NGF acute pain study and day 14 in the MIA chronic pain study; Fig. 1) or, in the case of the wheel running study, six days before imaging (one day before the commencement of the running wheel protocol). Rats were briefly anesthetised (3% isoflurane in 1 L/min oxygen and then maintained at 2.5% isoflurane). Once areflexic, a strip between the shoulder blades was shaved and then the skin swabbed with chlorhexidine and 5% lidocaine/prilocaine cream (EMLA; AstraZeneca, Macclesfield, UK) was applied topically. A small horizontal incision ( < 2 cm) was made between the shoulders and an osmotic pump was inserted and the skin sutured. Consistent with previous studies (Eschenko et al., 2010; Hoch et al., 2013) osmotic pumps had MR-compatible polyetheretherketone tubing (Alzet) and were loaded with saline or 80 mg/kg/200 μl $MnCl_2 \cdot (H_2O)2$ (equivalent

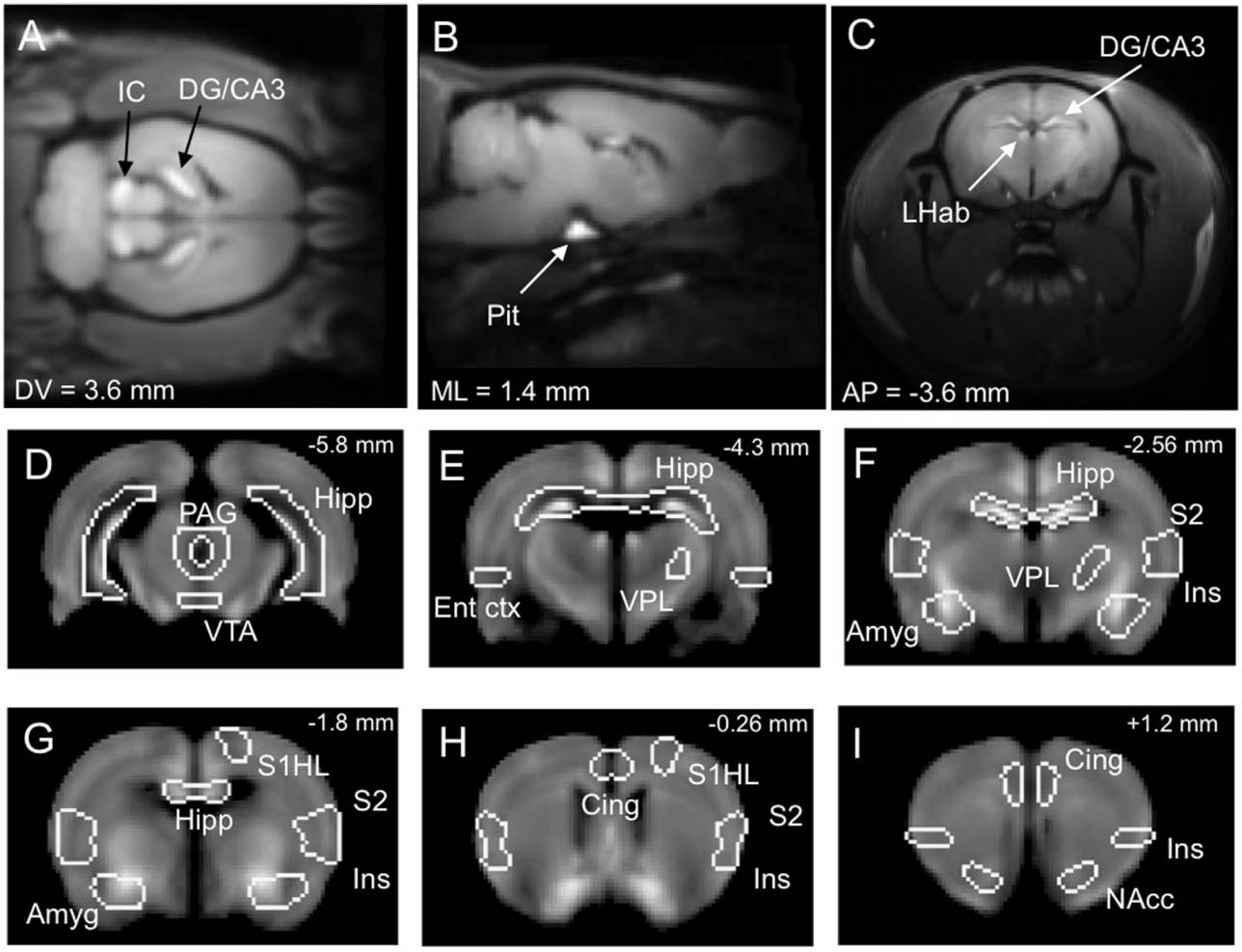


**Fig. 3.** Representative MDEFT images and indication of ROIs used to calculate average signal intensities. Following administration of $MnCl_2$ there was a heterogeneous signal distribution as shown in horizontal (A), sagittal (B) and coronal (C) planes of the rat brain. The selected ROIs are shown overlaid on MDEFT scans in coronal slices (posterior to anterior, D-I respectively). PAG: *peri*-aqueductal gray, VTA: ventral tegmental area, Hipp: hippocampus, VPL: ventroposterior lateral nucleus of the thalamus, Ent ctx: entorhinal cortex, S2: secondary somatosensory cortex, Ins: insula, Amyg: amygdala, S1HL: hindlimb primary somatosensory cortex, Cing: cingulate, NAcc: nucleus accumbens. Distances indicated are measurements from bregma according to the Paxinos & Watson rat brain atlas (Paxinos and Watson, 1998).

to an overall dose of 24 mg/kg $Mn^{2+}$ or 3.4 mg/kg/day $Mn^{2+}$; all doses refer to $MnCl_2{\cdot}(H_2O)2$ unless otherwise stated) in saline and released at a rate of 1 µl/h (0.4 mg/kg/µl). Osmotic pump action begins when the unit reaches body temperature; to ensure release immediately upon implantation, osmotic pumps were placed in a water bath heated to 37 °C the evening before implantation surgery.

MR relaxation rates are related to the local concentration of $Mn^{2+}$ and, therefore, sufficient amounts of $MnCl_2$ are necessary for detectable MRI contrast (Chuang et al., 2009; Silva and Bock, 2008). The upper dose of $MnCl_2$ that can be administered is limited due to toxicity and signal saturation. Toxic effects of $Mn^{2+}$ are reported at 5.5 mg/kg i.p. (administered as 20 mg/kg $MnCl_2{\cdot}(H_2O)4$ (Jackson et al., 2011)), though note that significant variation exists according to species and administration route (Boretius and Frahm, 2011). Signal saturation has been reported with the administration of 49.9 mg/kg $Mn^{2+}$ over 11 days (6 × 8.4 mg/kg $Mn^{2+}$ i.p. every 48 h equivalent to a daily dose of 4.2 mg/kg $Mn^{2+}$; re-calculated here as $Mn^{2+}$ but administered as $MnCl_2{\cdot}(H_2O)4$) (Bock et al., 2008; Silva and Bock, 2008). The dose used in our study, equivalent to 24 mg/kg $Mn^{2+}$ over seven days, has previously been validated by other groups and shown to produce sufficiently high local concentrations to generate good MRI contrast, enabling activity-dependent signal enhancement whilst avoiding $Mn^{2+}$ toxicity (Eschenko et al., 2010; Hoch et al., 2013).

To ensure that any potential effects of $MnCl_2$ on pain behaviour were identified, average pain behaviour measures in the week before (days 7 and 10) and after (days 14 and 17) osmotic pump implantation in MIA rats were compared.

### *MEMRI acquisition and analysis*

Imaging was performed on a 30 cm bore, 7 T MR scanner (Bruker Biospec 70/30) using a Bruker Avance III console (Bruker BioSpin, Ettlingen, Germany). Anaesthesia was induced with 3–5% isoflurane in oxygen and maintained at 1–2%; respiration was monitored to provide an index of anaesthetic depth (Model 1032, SA Instruments, Stony Brook, USA) and body temperature was maintained at 37 ± 1 °C via a water-pump system connected to tubing embedded in the base of the rat cradle. Saline was constantly infused via a subcutaneous line at a rate of 2 ml/h. Data were recorded using a receive-only rat head coil in combination with a 72 mm volume coil for excitation. Coronal T2 scans (rapid acquisition with refocused echoes, RARE) were acquired with the following parameters: effective TE = 28.5 ms, echo train length = 8, repetition time (TR) = 8055 ms, number of signal averages = 4, field of view (FOV) = 48 × 48×32 mm, matrix = 256 × 256×64, voxel size = 0.1875 × 0.1875 × 0.5 mm. Relative uptake of $Mn^{2+}$ was measured with a modified driven equilibrium Fourier transform (MDEFT; (Canals et al., 2008)) T1 scan with parameters identical to those reported in Eschenko et al. (Eschenko et al., 2010), optimised in that study for the contrast-to-noise ratio in the thalamus after $Mn^{2+}$ accumulation following injection in the motor cortex: TE = 4 ms, TR

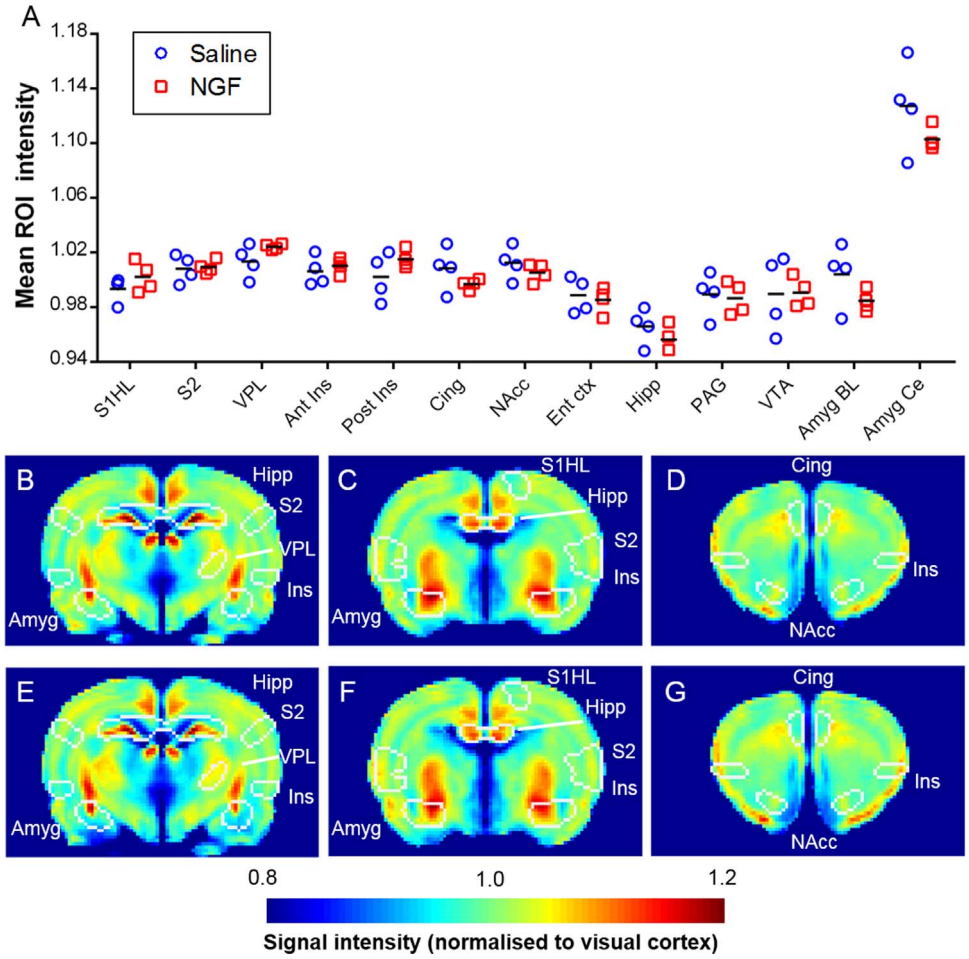


**Fig. 4.** Results of MEMRI scans in the acute pain, nerve growth factor (NGF) study. Average signal intensities for each ROI following two intra-articular injections of either NGF (10 μg/50 μl, n=4) or saline (50 μl, n=4). S1HL: hindlimb primary somatosensory cortex, S2: secondary somatosensory cortex, VPL: ventroposterior lateral nucleus of the thalamus, Ant Ins: anterior insula, Post Ins: posterior insula, Cing: cingulate, NAcc: nucleus accumbens, Ent ctx: entorhinal cortex, Hipp: hippocampus, PAG: *peri*-aqueductal gray, VTA: ventral-tegmental area, Amyg BL: basolateral amygdala, Amyg Ce: central nucleus of the amygdala. Average coronal brain images of all saline-injected (B-D, n=4) and NGF-injected animals (E-G, n=4) are shown. Images correspond to −3.3 mm (B, E), −1.8 mm (C, F), and +1.2 mm (D, G) with respect to bregma based on the Paxinos & Watson rat brain atlas (Paxinos and Watson, 1998). Colour bar represents normalised signal intensity.

= 22 ms, flip angle = 20°, inversion delay = 1000 ms. Coronal images were obtained with a FOV of 48 × 48×32 mm and a matrix size of 192 × 192×64, voxel size = 0.25 × 0.25 × 0.5 mm.

Two analyses of MEMRI data were performed: a region-based analysis using thirteen ROIs modified from the freely available Schwarz atlas (Schwarz et al., 2006), and a voxel-wise comparison. This combination of analyses has successfully been applied to similar MEMRI data sets by other groups (Bissig and Berkowitz, 2009; Hoch et al., 2013). Images were manually aligned to the Schwarz atlas and interpolated to identical dimensions (i.e. 96 × 96×30 voxels, 0.2 × 0.2 × 0.8 mm). MDEFT images in the coronal plane were rotated to the vertical and orthogonal to the horizontal planes using midline structures (e.g. third ventricle and the contact point between left and right retrospenial cortex) and sagittal slices rotated such that the dorsal surface of the inferior colliculus and olfactory bulbs were level (all rotations performed using ImageJ; v1.47, National Institute of Health, Bethesda, U.S.A.). Brains were roughly aligned to a standard brain size using the co-ordinates of dorsal, ventral and lateral extremes in two specific coronal slices using custom-written Matlab scripts (v2012 A; Natick, U.S.A.). Slices used to resize brains were those that most closely corresponded to atlas images (Paxinos and Watson, 1998) at −3.6 mm (identified by the anterior-most appearance of the lateral ventricles) and +1.6 mm (the anterior-most formation of the corpus callosum, i.e. the genu) with respect to bregma. Images were then trimmed and interpolated between slices that corresponded to −8.72 mm (opening of the fourth ventricle) and +3.2 mm (separation of the olfactory ventricle and forceps minor of the corpus callosum). The broad signal intensity gradient was corrected using the bias field correction utility in SPM8 (Wellcome Trust Centre for Neuroimaging, University College London, London, UK) using medium bias regularisation, 40 mm FWHM Gaussian smoothness (dimensions of voxels were increased by an order of magnitude in SPM functions). In order to ensure standardised ROIs were applicable to all individual brains, an average brain was produced from all brains and all individual brains aligned to the average brain using the *Normalisation* function within SPM8 (restricted to slices between −6.7 and 2.2 mm with respect to bregma).

As is customary in MEMRI analyses, each brain underwent tissue normalisation to the average signal of a region which was not expected to be activated in the two pain models (Eschenko et al., 2010; Yu et al., 2005; Bissig and Berkowitz, 2009); in the current study, signal was normalised to bilateral visual cortex. In the region-based analysis, average signal intensities were extracted for the following ROIs that have previously been implicated in acute and/or chronic pain (Mao et al., 1993): hindlimb primary somatosensory cortex (S1HL, contralateral to injection), secondary somatosensory cortex (S2), ventroposterior lateral nucleus of the thalamus (VPL; the hindlimb somatosensory area of the thalamus, contralateral to injection), anterior and posterior insula, cingulate (rat areas cg1 and cg2 encompassing areas equivalent to human anterior cingulate), nucleus accumbens (NAcc), entorhinal cortex, hippocampus (Hipp), *peri*-aqueductal gray (PAG)

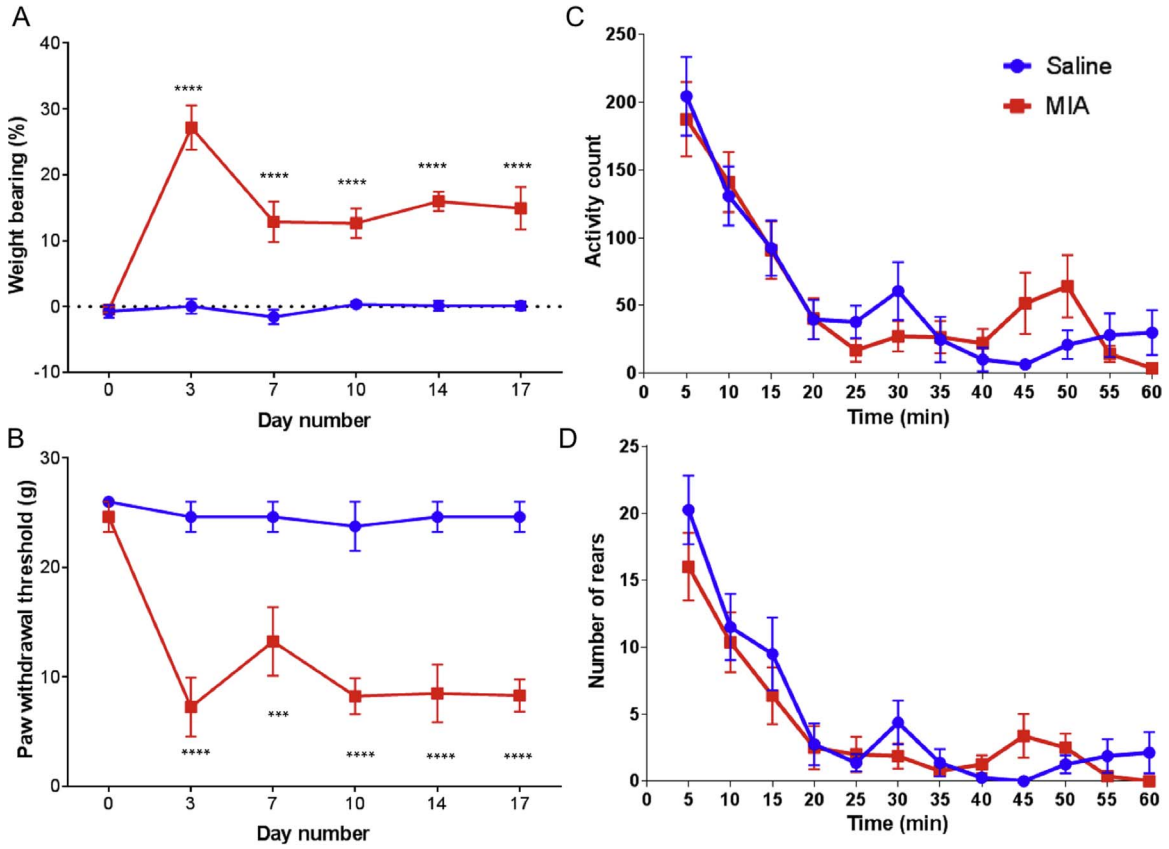


**Fig. 5.** Pain behaviour was measured immediately before and up to 17 days after intra-articular injection of MIA (1 mg/50 μl, n=8) or saline (50 μl, n=8). (A) There was a significant weight bearing asymmetry at all time points after injection of MIA compared to injection of saline. (B) Hindpaw withdrawal thresholds were significantly lowered at all time points following MIA injection, compared to saline. Locomotor activity was measured 17 days after intra-articular injection of MIA or saline, 3 days after commencement of $MnCl_2$ administration via osmotic pump. Activity counts (C; two consecutive beam breaks) and rearing (D; single interruption of upper beam breaks) was measured in 5 min bins. There was no difference in locomotor activity between rats which received intra-articular injection of MIA versus saline. All data were analysed using two-way ANOVAs (drug x time) and Sidak's multiple comparison post-hoc test; error bars represent standard error of the mean; *** $p < 0.001$, **** $p < 0.0001$.

and ventral-tegmental area (VTA), and the basolateral (BL) and central nucleus (Ce) of the amygdala. For the running wheel study, a combined sensorimotor ROI comprising the VPL and sensorimotor cortex (primary and secondary motor cortex, and hindlimb and forelimb primary somatosensory cortex) was used.

### *Statistical analysis*

Behavioural data (PWT, weight bearing, locomotor activity and rearing) were analysed with repeated measures two-way ANOVAs (drug x time) while any effect of $MnCl_2$ on pain behaviour measures were analysed with a paired *t*-test for weight bearing data and a non-parametric Wilcoxon matched-pairs signed rank test for PWT data. Region-based MEMRI data in the NGF and MIA pain model studies were analysed with ordinary two-way ANOVAs (drug x region) followed by Sidak's multiple comparison post-hoc tests. In the voxel-wise MEMRI analysis, statistical maps were generated in SPM8 using an unpaired *t*-test design between pain model and control brains with a p value threshold of 0.05 (family-wise error, FWE) with a minimum threshold cluster size of k=5. This was constrained to search only within the ROIs listed above by using a combined, binarised mask of all ROIs. Linear regression was performed on PWT or WB and MEMRI ROI intensities using animals from both pain models combined. We also ran a voxelwise regression analysis to identify whether behavioural indices of ongoing pain and hyperalgesia (WB scores and PWT respectively) were locally associated with the extent of MEMRI signal enhancement across both pain models. This analysis was constrained to within the pain processing areas using the binarised combined ROI mask from the group analysis and a FWE-corrected threshold of $p < 0.05$, $k > 5$. MEMRI data in the running wheel study (i.e. average intensity from a single sensorimotor ROI) was analysed with an unpaired *t*-test. A linear regression was performed in the wheel running study between the total running distance and MEMRI ROI intensity from the sensorimotor ROI. Data points were removed from a group and excluded from analysis if greater than > 2 standard deviations from the mean (considered a statistical outlier). With exception of the voxel-wise analysis, all statistical analyses were performed in Prism (v6.05; Graphpad, La Jolla, USA). All data are given as mean ± standard error of the mean.

## Results

### *NGF-injected rats: Pain behaviour*

Intra-articular injection of NGF produced a shift in weight distribution to the uninjured limb which was significantly different to saline-injected rats on all days tested post-injection (Fig. 2A; significant interaction between drug and time, $F_{3,18} = 13.59$, $p < 0.0001$). Average weight distribution on the final day of behavioural assessment before imaging (day 4) for saline and NGF-injected rats was −1.5 ± 1.2% and 20.0 ± 5.2%, respectively. NGF-injected rats did not exhibit a significant difference in PWTs, compared to saline-injected rats (Fig. 2B).

### *NGF-injected rats: MEMRI*

All acquired brain images exhibited regional heterogeneity in signal distribution typical of $MnCl_2$ administration; high signal intensities

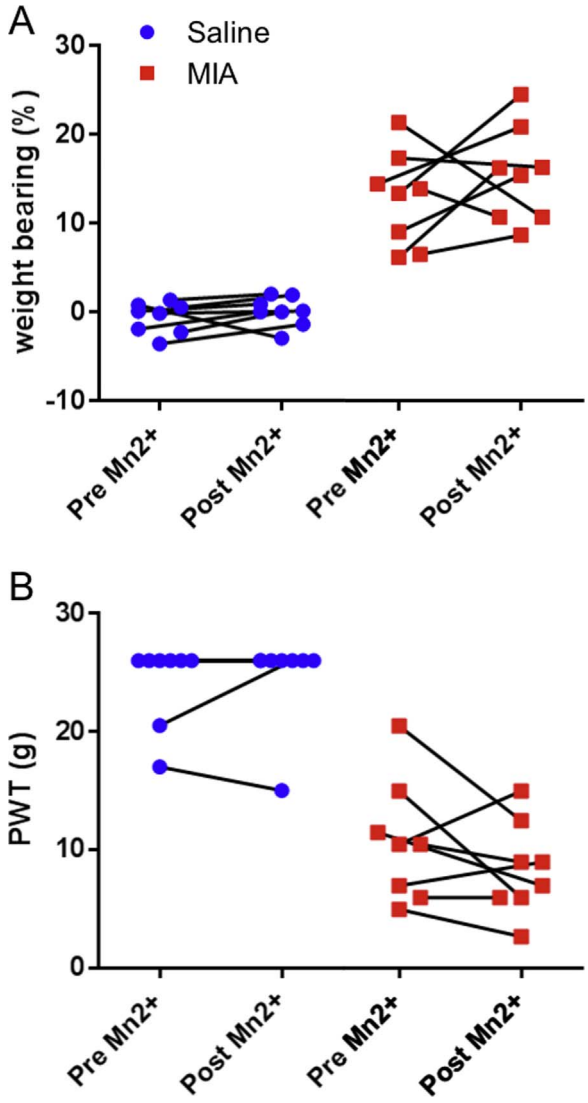


**Fig. 6.** Comparison of weight bearing asymmetry (A) and hindpaw withdrawal thresholds (B) before (average of day 7 and 10) and after (average of day 14 and 17) the seven day period of $MnCl_2$ (80 mg/kg) administration by implanted osmotic pump. Paired data are indicated with solid black lines. Exposure to $MnCl_2$ did not influence pain behaviour in rats that received intra-articular injection of MIA (1 mg/50 µl, n=8) or saline (50 µl, n=8).

were present in inferior colliculus, hippocampal dentate gyrus/cornu ammonis 3 (CA3), pituitary gland, and lateral habenula (Fig. 3A–C). Fig. 3D–I illustrates the ROIs from which average signal intensity was extracted (several ROIs extend over several slices). Following two intra-articular injections of either saline or NGF in the five days before scanning, there were no differences in signal intensity between saline- and NGF-treated rats in any of the structures examined (no interaction between drug and region, $F_{12,78} = 1.31$, $p = 0.23$; Fig. 4A). Three slices are shown from saline- (Fig. 4B–D) and NGF-injected rats (Fig. 4E–G) that indicate average signal intensities. Across brain regions there were marked differences in signal intensities (significant effect of region, $F_{12,78} = 52.74$, $p < 0.0001$); the Ce amygdala and hippocampus exhibited the largest and smallest signals, respectively (average of saline-treated animals for the Ce amygdala and hippocampus was: 1.127 ± 0.017 and 0.966 ± 0.007; average of NGF-treated animals was 1.103 ± 0.004 and 0.956 ± 0.005). The voxel-wise analysis performed between the two groups failed to detect any difference between voxel intensities (using a threshold of $p < 0.05$).

*MIA-injected rats: Behaviour*

Consistent with previous studies, intra-articular injection of MIA produced a shift in weight distribution to the uninjured limb which was significantly different to saline-injected rats on all days tested post-injection (Fig. 5A; significant interaction between drug and time, $F_{5,70} = 10.95$, $p < 0.0001$). Average weight distribution on the final day before imaging (day 17) for saline and MIA-injected rats was 0.1 ± 0.6% and 15 ± 3%, respectively. MIA-injected rats also exhibited a significant decrease in PWTs compared to saline-injected rats (Fig. 5B; significant interaction between drug and time, $F_{5,70} = 7.36$, $p < 0.0001$). Average PWT on the final day before imaging (day 17) for saline and MIA-injected rats were 24.6 ± 1.4 g and 8.3 ± 1.5 g, respectively. Any potential effects of $MnCl_2$ administration on locomotor activity, which would confound pain behaviour in the MIA group, were assessed by the measurement of spontaneous horizontal and vertical (rearing) activity on day 17. The profile of locomotor activity of MIA and saline-inject rats receiving $MnCl_2$ administration was comparable between the two groups (Figs. 5C and D). Paired analysis (Wilcoxon *t*-test), confirmed that pain behaviour remained stable between the days before (days 7 and 10) and after (days 14 and 17) surgery to implant the osmotic pump and the commencement of $MnCl_2$ administration (Figs. 6A, B).

*MIA-injected rats: MEMRI*

Scans took place 21 days following intra-articular injection of either saline or MIA at a time when differences in pain behaviour were robust and stable. There were no differences in signal intensity between saline- and MIA-treated rats in any of the ROIs (no interaction between drug and region, $F_{12,182} = 0.465$, $p = 0.93$; Fig. 7A). Three slices are shown from saline- (Fig. 7B–D) and MIA-injected rats (Fig. 7E–G) that indicate average signal intensities. As in the scans of NGF-treated rats, signal intensities differed between ROIs (significant effect of region, $F_{12,182} = 134.1$, $p < 0.0001$) with the Ce amygdala and hippocampus exhibiting the largest and smallest signals, respectively (average of saline-treated animals for the Ce amygdala and hippocampus was: 1.118 ± 0.007 and 0.970 ± 0.004; average of MIA-treated animals was 1.125 ± 0.008 and 0.975 ± 0.007). The voxel-wise analysis also failed to detect any group difference between voxel intensities (using a threshold of $p < 0.05$).

*Correlations of pain behaviour and MEMRI signal intensity*

To further explore any potential relationships between pain behaviour and $MnCl_2$ accumulation, data from the NGF and MIA treatment groups were combined (n=12) and potential correlations investigated between WB or PWT and regional signal intensity. Behavioural data used were the average for the periods of maximal pain behaviour (MIA model: days 14 and 17; NGF model days 1, 3 and 4). Signal intensity, based on $MnCl_2$ accumulation, was positively correlated with PWTs in the VTA ($R^2 = 0.37$, $F_{1,9} = 5.23$, $p < 0.05$) and negatively correlated with weight bearing differences in the VTA ($R^2 = 0.43$; $F_{1,10} = 7.48$, $p < 0.05$), the right Ce amygdala ($R^2 = 0.42$, $F_{1,10} = 7.10$, $p < 0.05$), and the left cingulate ($R^2 = 0.41$, $F_{1,10} = 6.82$, $p < 0.05$) (Fig. 8). No significant associations were identified using voxelwise regression analyses in the combined pain model groups.

*Voluntary wheel running MEMRI data*

Six days following the implantation of the osmotic pump and 9–16 h after the final wheel running session rats underwent imaging. Average MEMRI signal intensity in the sensorimotor ROI (normalised to visual cortex) in the control and running groups was 0.969 ± 0.003 and 0.976 ± 0.007, respectively; there was no difference between the two groups ($t_{13} = 1.091$, $p = 0.30$, n= 8 per group). However, regression

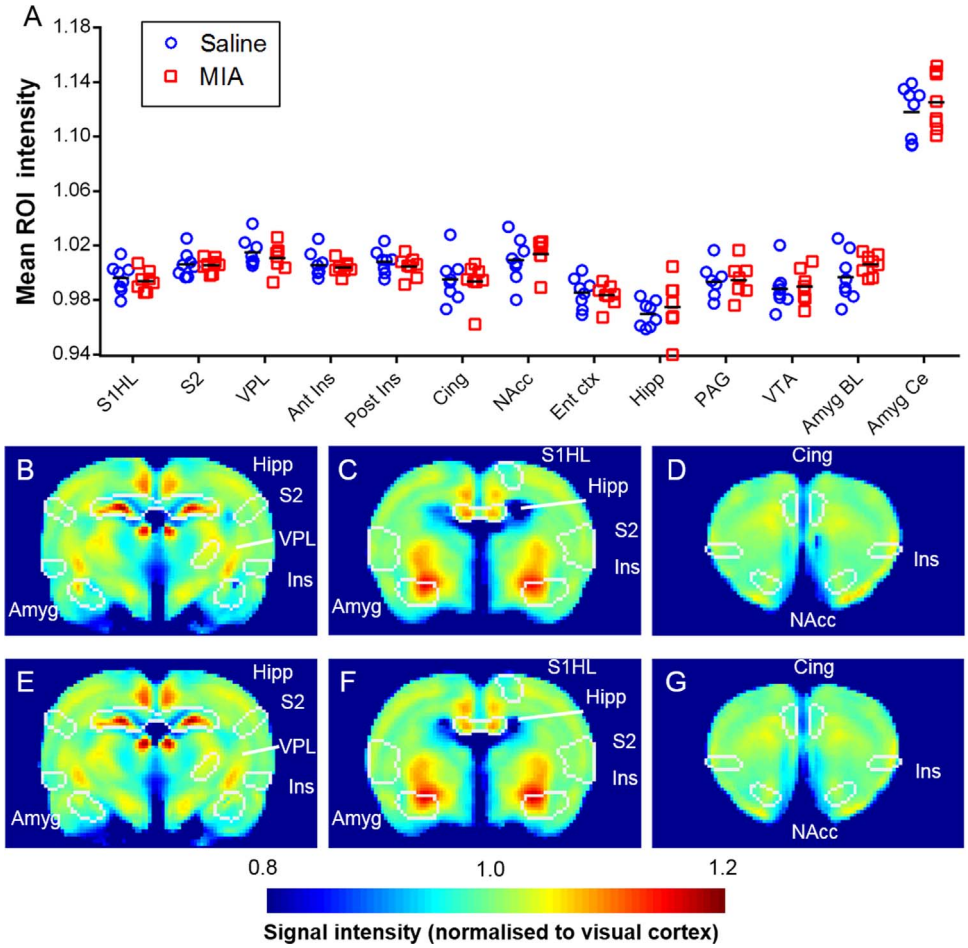


**Fig. 7.** Results of MEMRI scans in the chronic pain, monosodium iodoacetate (MIA) study. (A) Average signal intensities for each ROI 17 days after intra-articular injection of MIA (1 mg/50 μl, n=8) or saline (50 μl, n=8). Data were normalised to bilateral visual cortex. S1HL: hindlimb primary somatosensory cortex, S2: secondary somatosensory cortex, VPL: ventroposterior lateral nucleus of the thalamus, Ant Ins: anterior insula, Post Ins: posterior insula, Cing: cingulate, NAcc: nucleus accumbens, Ent ctx: entorhinal cortex, Hipp: hippocampus, PAG: *peri*-aqueductal gray, VTA: ventral-tegmental area, Amyg BL: basolateral amygdala, Amyg Ce: central nucleus of the amygdala. Average coronal brain images of all saline-injected (B-D, n=8) and MIA-injected animals (E-G, n=8) are shown. Images correspond to −3.3 mm (B, E), −1.8 mm (C, F), and +1.2 mm (D, G) with respect to bregma based on the Paxinos & Watson rat brain atlas (Paxinos and Watson, 1998). Colour bar represents normalised signal intensity.

analysis revealed a significant correlation between the average signal intensity of the sensorimotor ROI and the distance ran by each rat (Fig. 9; $R^2 = 0.5946$; $F_{1,5} = 7.332$; $p < 0.05$).

## Discussion

The aim of the current study was to evaluate the utility of MEMRI to study spontaneous pain and hyperalgesia in models of acute and chronic pain of the knee joint. The success of the two models, which consisted of intra-articular injection of the pro-nociceptive molecule NGF or the chondrocyte toxin MIA, was confirmed using established behavioural measures of pain that confirmed the presence of on-going pain and hyperalgesia, as indicated by changes in WB and PWTs, respectively. Although comparison between the respective control groups and the pain models did not reveal any significant differences in regional uptake of $MnCl_2$, we did reveal a significant inverse relationship between a behavioural index of on-going pain and $MnCl_2$ uptake in the VTA, right amygdala, and left cingulate and a positive correlation between $MnCl_2$ uptake in the VTA and PWTs.

The rationale for our study was to attempt to address the over-emphasis of previous preclinical imaging studies on evoked pain responses in models of either acute or chronic pain, which is often proposed as one of the reasons that these models have poor translational validity. Due to the sensitivity of functional activation patterns to anaesthesia (Thompson et al., 2014) it was also important in the current study that activity levels acquired from the brain represented those in the awake state. Given the technical demands and limited availability of PET scanners, in addition to their low spatial resolution, we evaluated an MR-based technique of acquiring waking-state brain activity levels. MEMRI produces activation maps that represent calcium uptake, which is dependent on the region's neuronal density, calcium channel density and distance from ventricular space. Over time, trans-synaptic axonal transport also influences regional distribution patterns (Boretius and Frahm, 2011). Slow administration of $MnCl_2$ is highly suitable for acquiring a surrogate measure of activity associated with a long-term stimulations such as auditory stimulation (Yu et al., 2005), visual stimulation (Bissig and Berkowitz, 2009), nutritional intake (Hoch et al., 2013), ageing (Bissig and Berkowitz, 2014), excitotoxicity (Gobbo et al., 2012), and, theoretically, spontaneous pain.

Our study replicated the methodology previously used to demonstrate increased MEMRI signal in primary motor and somatosensory cortex following voluntary wheel running (Eschenko et al., 2010). Consistent with previous studies (Boretius and Frahm, 2011; Lee et al., 2005) we obtained reliable brain activation maps using MEMRI with a typical heterogeneity between regions for our different experimental groups. Different from a previous MEMRI study showing differences in neuropathic and sham rats after a single bolus injection of $MnCl_2$ (Behera et al., 2013), we did not find group differences between pain models and controls using regional or voxel-based analysis.

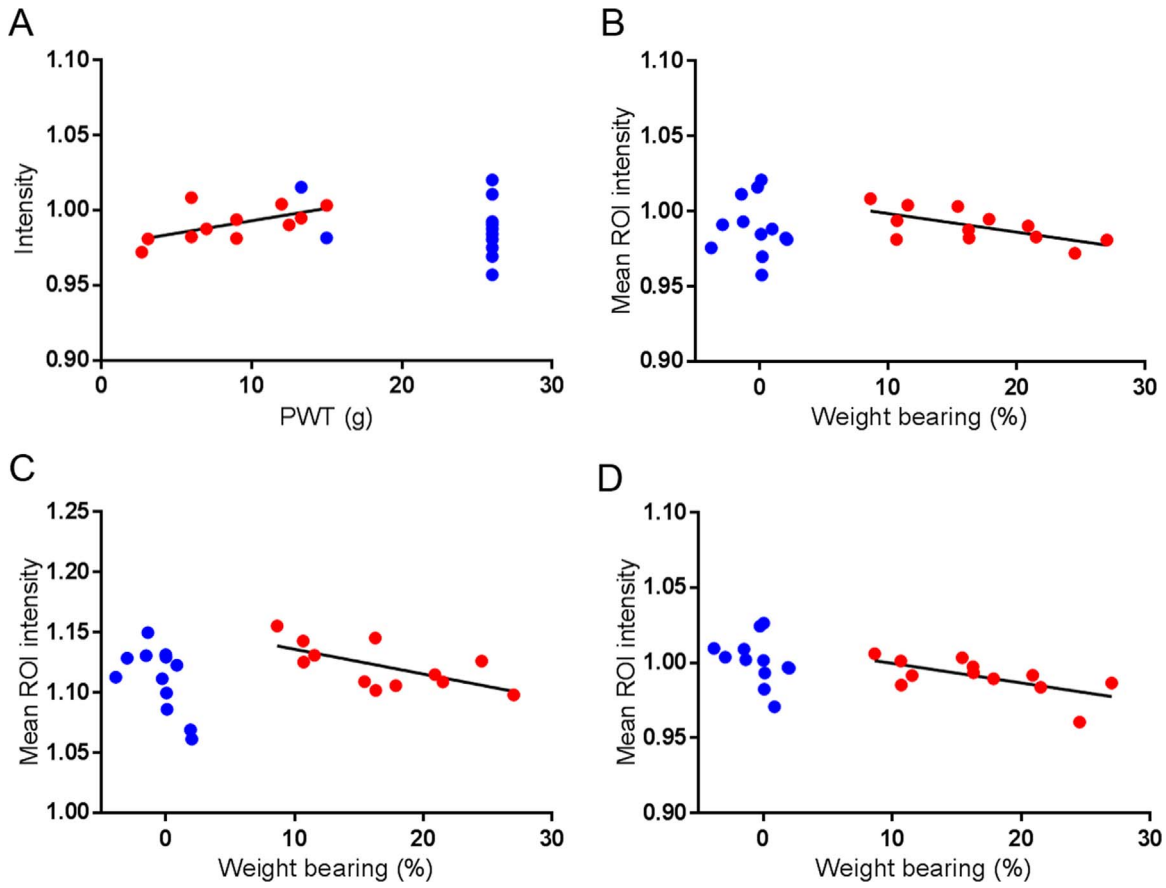


**Fig. 8.** Correlation between mean ROI intensity and paw-withdrawal thresholds (PWT, n=11) and weight bearing (n=12) using combined data from NGF and MIA injection studies. Data from animals in NGF and MIA groups are shown in red, control animals in blue. A: ventral tegmental area (with PWT data; $R^2 = 0.37$, $F_{1,9} = 5.23$, $p < 0.05$); B: ventral tegmental area (with weight bearing data; $R^2 = 0.43$, $F_{1,10} = 7.48$, $p < 0.05$); C: right-side central nucleus of the amygdala (with weight bearing data $R^2 = 0.42$, $F_{1,10} = 7.10$, $p < 0.05$); D: left-side cingulate (with weight bearing data $R^2 = 0.41$, $F_{1,10} = 6.82$, $p < 0.05$). Note for panel A that lower PWT value indicates more hyperalgesia; for panel B-C higher weight bearing % indicates higher pain behaviour.

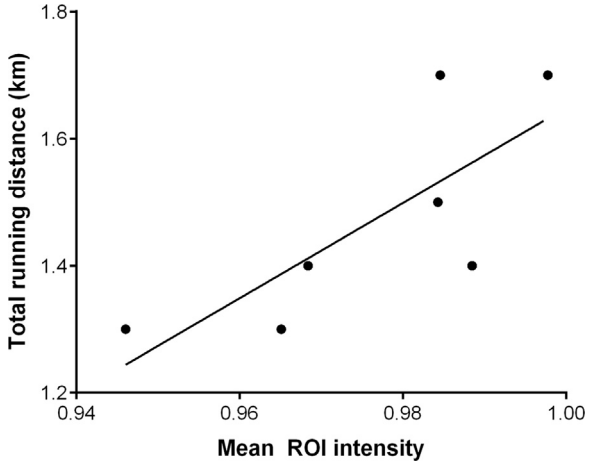


**Fig. 9.** Correlation between mean ROI intensity and total running distance. Data are total running distance over the previous five days against the average signal intensity of the sensorimotor cortex and VPL thalamus combined (normalised to bilateral visual cortex). Regression analysis shows that there is a significant deviation from 0 ($R^2 = 0.5946$, $p < 0.05$, $n = 7$). Data from one rat was a statistical outlier and was excluded from analysis.

Nevertheless, we found moderate correlations of MEMRI signal and pain behaviour suggesting that our MEMRI experiment had less sensitivity, only allowing us to detect within group inter-individual differences. To confirm this interpretation, we undertook an independent experiment repeating the locomotor intervention as in (Eschenko et al., 2010). We demonstrated a significant correlation between $MnCl_2$ uptake in sensorimotor regions (cortex and thalamus) and locomotor activity over the previous 7 days, but as in our pain study did not detect between group differences (running vs. not running rats). However, whilst we closely replicated the experimental paradigm in Eschenko et al., 2010, our rats did not run as far over the course of the study (between 1.3 and 1.7 km versus approximately 4 km total distance), which likely accounts for this difference. Indeed, the effect of wheel running on functional and structural connectivity is well documented, causing increased grey matter volume in motor and somatosensory cortex (Sumiyoshi et al., 2014), as well as more global trophic effects (Kempermann et al., 2010).

Although the sensitivity of MEMRI in absolute neural terms, for example regional metabolism or spike rate, is unknown, both stimulus intensity and duration can modulate overall MEMRI signal. Robust pain behaviour, in particular altered weight bearing (an index of ongoing pain), was evident throughout the period of delivery of $MnCl_2$ in the present study. Although MEMRI did not detect increases in $MnCl_2$ uptake in brain regions known to be activated by noxious stimuli, we did however detect significant correlations between decreases in $MnCl_2$ uptake in brain regions associated with fear, reward and avoidance and greater pain behaviour. Herein we report that $MnCl_2$ accumulation in the VTA, right Ce amygdala, and left cingulate was negatively correlated with pain responses (greater differences in weight bearing). Similarly $MnCl_2$ accumulation was reduced in the VTA in line with

hyperalgesia (lower PWTs). These data suggest reduced discrete regional activation as a result of the intensity and duration of pain experienced during the 7 days of $MnCl_2$ exposure. Our findings are consistent with decreased c-Fos activation in the VTA (Narita et al., 2003) and decreased overall dopamine levels and striatal D2 receptors in an animal model of chronic pain (Chang et al., 2014; Taylor et al., 2014). Experimental studies support a role of the VTA in the regulation of nociceptive responses (Li et al., 2016; Saadé et al., 1997; Sotres-Bayón et al., 2001; Takeda et al., 2005) and inhibition of dopamine neurones in the VTA encodes negative emotional signals, predicting aversive events in the environment (Mileykovskiy and Morales, 2011). Dopaminergic activation is not likely to occur during chronic pain states (Baliki and Apkarian, 2015; Vachon-Presseau et al., 2016) and both animal and human studies suggest that hypodopaminergic tone associated with chronic pain impairs motivated behaviour (Taylor et al., 2016).

Asymmetry of amygdala involvement in chronic pain is established, with right amygdala exhibiting a clearer association (Sadler et al., 2017). Whilst many studies have found amygdala neurons to increase activity during chronic pain states, there are many methodological disparities between different experimental paradigms or clinical conditions; and decreases in amygdala activation such as we show in the present study have been observed (Becerra et al., 1999), especially when the responses to ranges of pain intensities were measured (Derbyshire et al., 1997). FMRI studies of conditioned fear circuits in awake rodents demonstrated activation of the amygdala (Harris et al., 2015; Brydges et al., 2013), but reduced amygdala activity was reported in the unpaired group (Harris et al., 2015). Although the role of anterior cingulate in emotional / aversive aspects of pain processing is established (Johansen et al., 2001), future MEMRI studies could investigate further the influence of on-going pain behaviour and conditioned place avoidance paradigms. Our demonstration of an association between a reduction in $MnCl_2$ accumulation in discrete brain regions and pain behaviour in the models of on-going pain further reveal the complexities of brain networks altered under these conditions, and suggests that MEMRI may help to unravel the interplay between fear, reward and avoidance behaviour in the context of pain.

Comparison of our findings using MEMRI and our earlier BOLD imaging study of brain regional responses (Abaei et al., 2016) reveals marked differences in the alterations in brain networks following 7 days of on-going pain behaviour versus the response of brain networks following activation of nociceptive pathways in the same model of pain under anaesthesia. Noxious stimulation of the MIA knee induced a significantly greater increase in functional connectivity in the mediodorsal thalamic nucleus, hippocampus, and globus pallidus, compared to noxious stimulation of the control knee (Abaei et al., 2016). Other studies using the MIA model predominantly focused on alterations in spinal nociceptive responses, such as reflex pathways (Kelly et al., 2015), increased neuronal responses (Sagar et al., 2010) and c-Fos expression in the spinal cord (Ogbonna et al., 2013), all indicating an activation of nociceptive pathways.

In conclusion, the moderate regional-specific correlations of MEMRI signal and pain behaviour reported herein indicate that in vivo MEMRI at 7 T is sensitive to cumulative neural effects of pain behaviour in awake freely moving animals. Further improvements to MEMRI will arise from recent and ongoing refinement of safe manganese doses (Gálosi et al., 2017; Poole et al., 2017), as well as the use of post-mortem scanning (enabling a longer scan time and therefore resolution) where experimental paradigms allow (Sperry et al., 2017). These developments, combined with an increase of signal to noise ratios through use of optimised acquisition hardware (field strength, dedicated coils), may improve the sensitivity of MEMRI to strengthen future investigations into the neural mechanisms underpinning spontaneous pain in rats. The potential key impact will come from overcoming the reliance of preclinical imaging studies on evoked pain responses in models of either acute or chronic pain.

## Acknowledgements

We would like to thank Arthritis Research UK for funding this work (grant number 18769), and Clare Spicer (University of Nottingham) for technical expertise.

## References

Abaei, M., et al., 2016. Neural correlates of hyperalgesia in the monosodium iodoacetate model of osteoarthritis pain. Mol. Pain. 12 (0).
Ashraf, S., et al., 2014. Augmented pain behavioural responses to intra-articular injection of nerve growth factor in two animal models of osteoarthritis. Ann. Rheum. Dis. 73 (9), 1710–1718.
Baliki, M.N., Apkarian, A.V., 2015. Nociception, pain, negative moods, and behavior selection. Neuron 87 (3), 474–491.
Becerra, L.R., et al., 1999. Human brain activation under controlled thermal stimulation and habituation to noxious heat: an fMRI study. Magn. Reson. Med. 41 (5), 1044–1057.
Behera, D., et al., 2013. Bilateral peripheral neural activity observed in vivo following unilateral nerve injury. Am. J. Nucl. Med. Mol. Imaging 3 (3), 282–290 https://www.ncbi.nlm.nih.gov/pubmed/23638339.
Bissig, D., Berkowitz, B.A., 2009. Manganese-enhanced MRI of layer-specific activity in the visual cortex from awake and free-moving rats. NeuroImage 44 (3), 627–635.
Bissig, D., Berkowitz, B.A., 2014. Testing the calcium hypothesis of aging in the rat hippocampus in vivo using manganese-enhanced MRI. Neurobiol. Aging 35 (6), 1453–1458.
Bock, N.A., Paiva, F.F., Silva, A.C., 2008. Fractionated manganese-enhanced MRI. NMR Biomed. 21 (5), 473–478.
Boretius, S., Frahm, J., 2011. Manganese-enhanced magnetic resonance imaging. Methods Mol. Biol. 771, 531–568.
Borsook, D., Becerra, L., 2011. CNS animal fMRI in pain and analgesia. Neurosci. Biobehav. Rev. 35 (5), 1125–1143.
Brydges, N.M. et al., 2013. Imaging conditioned fear circuitry using awake rodent fMRI. Y. Herault, ed. PLoS One, 8(1), e54197.
Canals, S., et al., 2008. Magnetic resonance imaging of cortical connectivity in vivo. NeuroImage 40 (2), 458–472.
Chang, P.-C., et al., 2014. Role of nucleus accumbens in neuropathic pain: linked multi-scale evidence in the rat transitioning to neuropathic pain. Pain 155 (6), 1128–1139.
Chaplan, S.R., et al., 1994. Quantitative assessment of tactile allodynia in the rat paw. J. Neurosci. Methods 53 (1), 55–63.
Chuang, K.-H., Koretsky, A.P., Sotak, C.H., 2009. Temporal changes in the T1 and T2 relaxation rates (DeltaR1 and DeltaR2) in the rat brain are consistent with the tissue-clearance rates of elemental manganese. Mag. Reson. Med. 61 (6), 1528–1532.
Combe, R., Bramwell, S., Field, M.J., 2004. The monosodium iodoacetate model of osteoarthritis: a model of chronic nociceptive pain in rats? Neurosci. Lett. 370 (2–3), 236–240.
Cottam, W.J., et al., 2016. Associations of limbic-affective brain activity and severity of ongoing chronic arthritis pain are explained by trait anxiety. NeuroImage: Clin. 12, 269–276.
Derbyshire, S.W., et al., 1997. Pain processing during three levels of noxious stimulation produces differential patterns of central activity. Pain 73 (3), 431–445.
Eschenko, O., et al., 2010. Mapping of functional brain activity in freely behaving rats during voluntary running using manganese-enhanced MRI: implication for longitudinal studies. NeuroImage 49 (3), 2544–2555.
Gálosi, R., et al., 2017. Identifying non-toxic doses of manganese for manganese-enhanced magnetic resonance imaging to map brain areas activated by operant behavior in trained rats. Magn. Reson. Imaging 37, 122–133.
Gobbo, O.L., et al., 2012. In vivo detection of excitotoxicity by manganese-enhanced MRI: comparison with physiological stimulation. Mag. Res. Med. 68 (1), 234–240.
Guingamp, C., et al., 1997. Mono-iodoacetate-induced experimental osteoarthritis: a dose-response study of loss of mobility, morphology, and biochemistry. Arthritis Rheum. 40 (9), 1670–1679.
Harris, A.P., et al., 2015. Imaging learned fear circuitry in awake mice using fMRI. Eur. J. Neurosci. 42 (5), 2125–2134.
Hoch, T., et al., 2013. Manganese-enhanced magnetic resonance imaging for mapping of whole brain activity patterns associated with the intake of snack food in ad libitum fed rats. PLoS One 8 (2), e55354.
Howard, M.A., et al., 2011. Beyond patient reported pain: perfusion magnetic resonance imaging demonstrates reproducible cerebral representation of ongoing post-surgical painPLoS One 6, e17096, B. Baune, ed.
Jackson, S.J., et al., 2011. Manganese-enhanced magnetic resonance imaging (MEMRI) of rat brain after systemic administration of MnCl2: hippocampal signal enhancement without disruption of hippocampus-dependent behavior. Behav. Brain Res. 216 (1), 293–300.
Johansen, J.P., Fields, H.L., Manning, B.H., 2001. The affective component of pain in rodents: direct evidence for a contribution of the anterior cingulate cortex. Proc. Natl. Acad. Sci. USA 98 (14), 8077–8082.
Kelly, S., et al., 2015. Increased function of pronociceptive TRPV1 at the level of the joint in a rat model of osteoarthritis pain. Ann. Rheum. Dis. 74 (1), 252–259.
Kempermann, G., et al., 2010. Why and how physical activity promotes experience-induced brain plasticity. Front. Neurosci. 4, 189.
Kulkarni, B., et al., 2007. Arthritic pain is processed in brain areas concerned with emotions and fear. Arthritis Rheum. 56 (4), 1345–1354.

Lee, J.H., et al., 2005. Manganese-enhanced magnetic resonance imaging of mouse brain after systemic administration of MnCl2: dose-dependent and temporal evolution of T1 contrast. Mag. Reson. Med. 53 (3), 640–648.
Lee, M.C., Tracey, I., 2013. Imaging pain: a potent means for investigating pain mechanisms in patients. Br. J. Anaesth. 111 (1), 64–72.
Lewin, G.R., Lechner, S.G., Smith, E.S.J., 2014. Nerve growth factor and nociception: from experimental embryology to new analgesic therapyHandb. Exp. Pharmacol. 220, 251–282.
Li, A.-L., et al., 2016. Stimulation of the ventral tegmental area increased nociceptive thresholds and decreased spinal dorsal horn neuronal activity in rat. Exp. Brain Res. 234 (6), 1505–1514.
Mao, J., Mayer, D.J., Price, D.D., 1993. Patterns of increased brain activity indicative of pain in a rat model of peripheral mononeuropathy. J. Neurosci. 13 (6), 2689–2702.
Martin, C., et al., 2006. Investigating neural-hemodynamic coupling and the hemodynamic response function in the awake rat. NeuroImage 32 (1), 33–48.
Martin, C., 2014. Contributions and complexities from the use of in vivo animal models to improve understanding of human neuroimaging signals. Front. Neurosci. 8, 211.
Mileykovskiy, B., Morales, M., 2011. Duration of inhibition of ventral tegmental area dopamine neurons encodes a level of conditioned fear. J. Neurosci. 31 (20), 7471–7476.
Mok, S.I., Munasinghe, J.P., Young, W.S., 2012. Infusion-based manganese-enhanced MRI: a new imaging technique to visualize the mouse brain. Brain Struct. Funct. 217 (1), 107–114.
Narita, M., et al., 2003. Change in the expression of c-fos in the rat brain following sciatic nerve ligation. Neurosci. Lett. 352 (3), 231–233.
Ogbonna, A.C., et al., 2013. Pain-like behaviour and spinal changes in the monosodium iodoacetate model of osteoarthritis in C57Bl/6 mice. Eur. J. Pain 17 (4), 514–526.
Olanow, C.W., 2004. Manganese-induced parkinsonism and Parkinson's disease. Ann. N.Y. Acad. Sci. 1012, 209–223.
Parks, E.L., et al., 2011. Brain activity for chronic knee osteoarthritis: dissociating evoked pain from spontaneous pain. Eur. J. Pain. 15 (8), (843.e1-14).
Paxinos, G., Watson, C., 1998. The Rat Brain in Stereotaxic Coordinates. Academic Press, San Diego, USA.
Poole, D.S., et al., 2017. Continuous infusion of manganese improves contrast and reduces side effects in manganese-enhanced magnetic resonance imaging studies. NeuroImage 147, 1–9.
Saadé, N.E., et al., 1997. Augmentation of nociceptive reflexes and chronic deafferentation pain by chemical lesions of either dopaminergic terminals or midbrain dopaminergic neurons. Brain Res. 751 (1), 1–12.
Sadler, K.E., et al., 2017. Divergent functions of the left and right central amygdala in visceral nociception. Pain 158 (4), 747–759.
Sagar, D.R., et al., 2010. Tonic modulation of spinal hyperexcitability by the endocannabinoid receptor system in a rat model of osteoarthritis pain. Arthritis Rheum. 62 (12), 3666–3676.
Sagar, D.R., et al., 2014. Osteoprotegerin reduces the development of pain behaviour and joint pathology in a model of osteoarthritis. Ann. Rheum. Dis. 73 (8), 1558–1565.
Schwarz, A.J., et al., 2006. A stereotaxic MRI template set for the rat brain with tissue class distribution maps and co-registered anatomical atlas: application to pharmacological MRI. NeuroImage 32 (2), 538–550.
Silva, A.C., et al., 2004. Manganese-enhanced magnetic resonance imaging (MEMRI): methodological and practical considerations. NMR Biomed. 17 (8), 532–543.
Silva, A.C., Bock, N.A., 2008. Manganese-enhanced MRI: an exceptional tool in translational neuroimaging. Schizophr. Bull. 34 (4), 595–604.
Sotres-Bayón, F., et al., 2001. Lesion and electrical stimulation of the ventral tegmental area modify persistent nociceptive behavior in the rat. Brain Res. 898 (2), 342–349.
Sperry, M.M., et al., 2017. Mapping of pain circuitry in early post-natal development using manganese-enhanced MRI in rats. Neuroscience 352, 180–189.
Sumiyoshi, A., et al., 2014. Regional gray matter volume increases following 7days of voluntary wheel running exercise: a longitudinal VBM study in rats. NeuroImage 98, 82–90.
Takeda, R., et al., 2005. Unilateral lesions of mesostriatal dopaminergic pathway alters the withdrawal response of the rat hindpaw to mechanical stimulation. Neurosci. Res. 52 (1), 31–36.
Tanasescu, R., et al., 2016. Functional reorganisation in chronic pain and neural correlates of pain sensitisation: a coordinate based meta-analysis of 266 cutaneous pain fMRI studies. Neurosci. Biobehav. Rev. 68, 120–133.
Tappe-Theodor, A., Kuner, R., 2014. Studying ongoing and spontaneous pain in rodents–challenges and opportunities. Eur. J. Neurosci. 39 (11), 1881–1890.
Taylor, A.M.W., et al., 2014. Correlation Between Ventral Striatal Catecholamine Content and Nociceptive Thresholds in Neuropathic Mice. J. Pain. 15 (8), 878–885.
Taylor, A.M.W., et al., 2016. Mesolimbic dopamine signaling in acute and chronic pain: implications for motivation, analgesia, and addiction. Pain 157 (6), 1194–1198.
Thompson, S.J., et al., 2014. Metabolic brain activity suggestive of persistent pain in a rat model of neuropathic pain. NeuroImage 91, 344–352.
Thompson, S.J., Bushnell, M.C., 2012. Rodent functional and anatomical imaging of pain. Neurosci. Lett. 520 (2), 131–139.
Tracey, I., Bushnell, M.C., 2009. How neuroimaging studies have challenged us to rethink: is chronic pain a disease? Pain 10 (11), 1113–1120.
Vachon-Presseau, E., et al., 2016. The emotional brain as a predictor and amplifier of chronic pain. J. Dent. Res. 95 (6), 605–612.
Watson, D.J.G., et al., 2012. Blockade of dopamine D3 but not D2 receptors reverses the novel object discrimination impairment produced by post-weaning social isolation: implications for schizophrenia and its treatment. Int. J. Neuropsychopharmacol. 15 (4), 471–484.
Wolf, G.L., Baum, L., 1983. Cardiovascular toxicity and tissue proton T1 response to manganese injection in the dog and rabbit. Am. J. Roentgenol. 141 (1), 193–197.
Yu, X., et al., 2005. In vivo auditory brain mapping in mice with Mn-enhanced MRI. Nat. Neurosci. 8 (7), 961–968.